Available online at www.sciencedirect.com
SCIENCE DIRECT®
Journal of Nuclear Materials 342 (2005) 77–89
journal of nuclear materials
www.elsevier.com/locate/jnucmat

Microstructural behavior of VVER-440 reactor pressure vessel steels under irradiation to neutron fluences beyond the design operation period

E.A. Kuleshova [a,*], B.A. Gurovich [a], Ya.I. Shtrombakh [a], Yu.A. Nikolaev [a], V.A. Pechenkin [b]

[a] *Russian Research Center 'Kurchatov Institute', Kurchatov sq. 1, Moscow 123182, Russia*
[b] *State Scientific Center of Russian Federation, Institute of Physics and Power Engineering, Bondarenko sq. 1, Obninsk, Kaluga region 249033, Russia*

Received 15 March 2004; accepted 1 March 2005

Abstract

Electron-microscopy and fractographic studies of the surveillance specimens from base and weld metals of VVER-440/213 reactor pressure vessel (RPV) in the original state and after irradiations to different fast neutron fluences from $\sim 5 \times 10^{23}$ n m^{-2} ($E > 0.5$ MeV) up to over design values have been carried out. The maximum specimens irradiation time was 84 480 h. It is shown that there is an evolution in radiation-induced structural behavior with radiation dose increase, which causes a change in relative contribution of the mechanisms responsible for radiation embrittlement of RPV materials. Particularly, radiation coalescence of copper-enriched precipitates and extensive density increase of dislocation loops was observed. Increase in dislocation loop density was shown to provide the dominant contribution to radiation hardening at the late irradiation stages (after reaching double the design end-of-life neutron fluence of $\sim 4 \times 10^{24}$ n m^{-2}). The fracture mechanism of the base metal at those stages was observed to change from transcrystalline to intercrystalline.

1. Introduction

Rate and value of radiation embrittlement are known to be determined by only structural changes in the steel under irradiation. These changes depend on irradiation conditions and chemical composition as well as on structure of the steel. For an adequate understanding of different mechanisms contribution in radiation embrittlement of the steels irradiated to different fast neutron fluences (for the design operation period and beyond), the studies of the structural changes in the steels irradiated to fast neutron fluence beyond design operation period are necessary. Such studies allow more reliable validation of RPV materials workability during operation and also an estimation of safe life prolongation.

The set of effects observed during radiation embrittlement of RPV materials is stipulated, mainly, by joint action of three mechanisms: the hardening of steel under irradiation, the formation of intergranular impurity segregation, and also the occurrence of impurity

* Corresponding author.
E-mail address: evgenia-orm@yandex.ru (E.A. Kuleshova).

0022-3115/$ - see front matter © 2005 Elsevier B.V. All rights reserved.
doi:10.1016/j.jnucmat.2005.03.011

segregation to interface boundaries precipitates/matrix, i.e. the occurrence of intragranular impurity segregation [1–3]. It was shown [1] that at fast neutron fluence of $<10^{24}$ n m^{-2} (hereinafter fast neutron fluence is given with $E > 0.5$ MeV) radiation embrittlement for VVER-440/213 materials is originated mainly from two mechanisms: the hardening (yield strength increase) caused by the occurrence of radiation defects and radiation-induced precipitates, and also by the occurrence of intragranular phosphorus segregation to interface boundaries under irradiation. At such values of neutron fluence the third mechanism of radiation embrittlement of RPV steels – the occurrence of intergranular phosphorus segregation – is responsible, as a rule, for an insignificant part of radiation-induced shift of ductile-to-brittle transition (DBT) temperature, not more than ~10–20%, presumably [1,4].

With neutron fluence increase the relative contribution of different mechanisms to radiation embrittlement could be considerably changed, because of matrix depletion by the elements that form radiation-induced precipitates (that are a support for intragranular interface segregation). The data showing multi-stage character of radiation embrittlement for VVER-440 materials proves it [5–7].

According to the above-mentioned considerations the objective of the present work was a comparison of structural and fractographic studies for VVER-440 pressure vessel base and weld metals irradiated up to the fluence of 8.66×10^{24} n m^{-2} to obtain more adequate understanding of the mechanisms that determine radiation embrittlement of the steels at the stages beyond design operation period.

2. Materials and test methods

The base (15Kh2MFA) and the weld (Sv-10KhMFT) metals (Table 1) of VVER-440 reactor pressure vessel were studied.

The embrittlement of specimens after irradiation was estimated by ductile-to-brittle transition temperature shift and also by the decrease of the upper shelf energy (USE) level on the temperature dependence curve for impact tests.

The ductile to brittle transition temperature evaluated according to [8,9] was accepted as ductile-to-brittle transition temperature (DBTT). The evaluation technique of critical brittleness temperature is given in details in [10].

Broken halves of Charpy specimens were studied using fractography. To preserve their fracture surfaces they were selected and stored in vacuum immediately after testing.

The fracture surfaces were studied using an X-ray micro analyzer SXR-50 modified for radioactive examination ('Cameca' Co., France), and placed in a hot cell. Fracture images were obtained using secondary electrons at an accelerating voltage of 20 kV and a probe current of 0.8 nA in the magnification range 50–3500. The percentage of different fracture modes (ductile, brittle intergranular, ductile intergranular, cleavage and quasi-cleavage) in the total fracture surface after testing at different temperatures was estimated by Glagolev's method [11]. The absolute error of measuring at confidence level of 95% did not exceed 5%. The test temperatures for each material corresponded to: USE; DBTT and lower shelf energy (LSE) on the impact bend energy temperature dependence curve.

Transmission electron microscopy (TEM) studies were carried out using an electron microscope TEM-SCAN-200CX ('Jeol', Japan) at an accelerating voltage of 200 kV. The density of radiation defects and precipitates were estimated with a foil thickness measured using a convergent beam electron diffraction method [12], which provides an accuracy with errors less than 5%. The specimens for TEM-studies were cut out from the broken halves of Charpy specimens. Further preparation of specimens included electropolishing using a 'Struers' installation (Austria) at a temperature of −60 to −70 °C just before placing them in the microscope. The electrolyte composition for electropolishing was 10% HC1O4 +90% methanol.

3. Results

The investigated materials were exposed to neutron radiation in the surveillance channels of VVER-440/213 reactor pressure vessel at 270 °C and to thermal ageing at 290 °C. The results of mechanical tests for the materials studied are presented in Figs. 1–4.

As can be seen from Figs. 1 and 2, irradiation caused essential increase in yield strength and in critical brittleness temperature of the steel. The dose dependencies in Figs. 1 and 2 have a well defined multi-stage character.

Table 1
Chemical composition of the materials studied (wt%)

Material	Grade	C	Si	Mn	Cr	S	P	Cu	Mo	V
Base metal	15Kh2MFA	0.16	0.23	0.41	2.63	0.010	0.010	0.09	0.66	0.28
Weld metal	Sv-10KhMFT	0.05	0.29	0.87	1.53	0.005	0.010	0.03	0.48	0.48

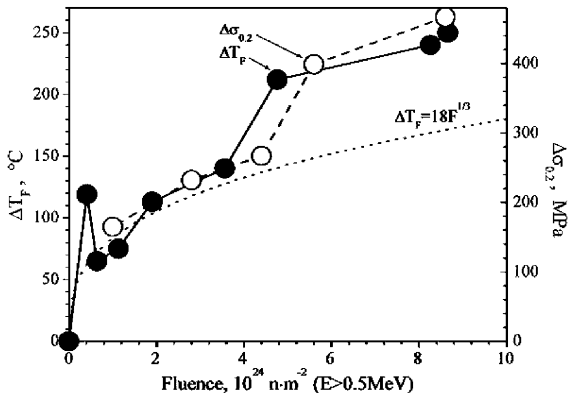

Fig. 1. Ductile-to-brittle transition temperature and yield strength of the base metal as a function of fast neutron fluence in comparison with the standard reference dependence specified for evaluation of radiation embrittlement for VVER-440 base metal ($\Delta T_F = 18F^{1/3}$) [8].

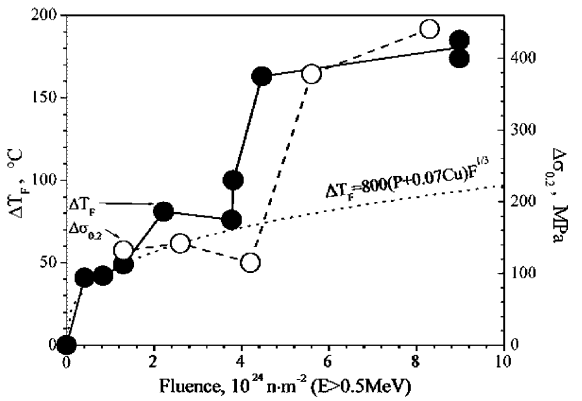

Fig. 2. Ductile-to-brittle transition temperature and yield strength of the weld metal as a function of fast neutron fluence in comparison with the standard reference dependence specified for evaluation of metal radiation embrittlement for VVER-440 weld metal ($\Delta T_F = 800(P + 0.07Cu)F^{1/3}$) [8].

At fluences above $(1–1.3) \times 10^{24}$ n m^{-2} the character of yield strength dose dependence has no formal correlation with transition temperature shift in the range of fluences, where yield strength decrease and DBTT growth (especially for weld metal) are observed. However, this important fact for understanding of the phenomenon nature needs additional explanation involving extra experimental data.

A comparison of the data given in Figs. 1 and 2 and the thermal ageing data given in Figs. 3 and 4 for the materials studied showed that changes in critical brittleness temperature and in yield strength caused by irradiation are much higher than the corresponding changes caused by thermal ageing. It should be noted that for

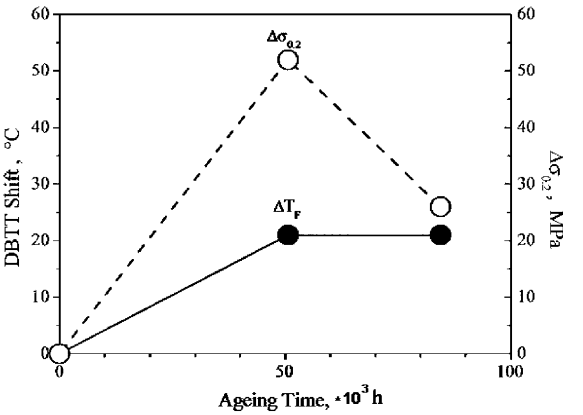

Fig. 3. Ductile-to-brittle transition temperature and yield strength of the base metal at thermal ageing at 290 °C.

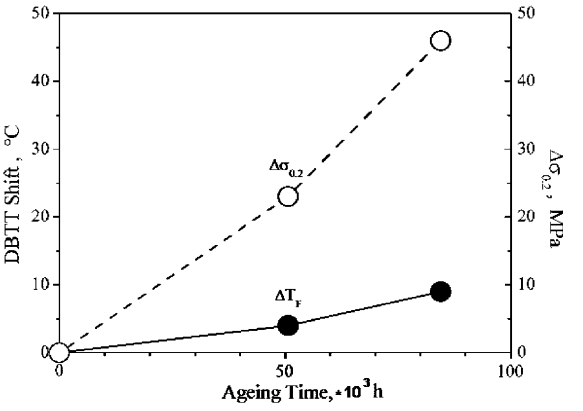

Fig. 4. Ductile-to-brittle transition temperature and yield strength of the weld metal at thermal ageing at 290 °C.

base metal there is an explicit overageing stage in a fluence range of $\sim(2–4) \times 10^{24}$ n m^{-2} (Fig. 3).

The results of fractographic studies of Charpy specimens from base metal in the initial condition, after irradiation at 270 °C to fluence 8.66×10^{20} n m^{-2} and after thermal ageing at 290 °C during 3520 days (84 480 h that corresponds to irradiation time of the specimens to the fluence 8.66×10^{24} n m^{-2}) are presented in Table 2. The results obtained allow a formulation of the following regularity concerning mode of fracture structure.

The quantitative processing of the fractographic results shows that the normalized values of absorbed energy – A/A_{us} (A – value of absorbed energy at particular temperature, A_{us} – upper shelf energy) correlate to the fraction of zones with ductile fracture mode in the total fracture surface under all the conditions and temperatures of impact tests.

In the initial condition there is small brittle intergranular fraction in the fractures of the specimens from base

Table 2
The results of fractographic studies of Charpy specimens of base and weld metals

Material	Condition, Fluence, 10^{24} n m^{-2}, DBTT	Specimen number	T_{test}, °C	Absorbed energy, J	Fraction of structural components in the fracture, %				
					Ductile	Quasi-cleavage	Cleavage	Brittle intergranular	Ductile intergranular
Base metal	Unirradiated, DBTT = −52 °C	1	−60	10	–	95	Traces	5	–
		2	−40	51	30	55	5	10	–
		3	100	187	100	–		–	
	Thermal aging at 290 °C during 84480 h, DBTT = −31 °C, $\Delta\sigma_{0.2}$ = 26 MPa	4	−100	4	–	90	5	5	–
		5	−40	13	5	70	5	20	–
		6	−40	41	20	60	5	15	–
		7	−20	70	35	50	5	10	–
	Irradiated, Fluence = 8.66, DBTT = 198 °C, $\Delta\sigma_{0.2}$ = 467 MPa	8	200	52	45	Traces	–	50	5
		9	220	39	30	–	–	65	5
		10	220	93	95	–	–	–	5
Weld metal	Unirradiated, DBTT = 8 °C	11	−20	13	5	90	5	–	–
		12	0	27	15	80	5	–	–
		13	20	63	40	50	10	–	–
		14	100	129	100	–	–	–	–
	Irradiated, Fluence = 8.98, DBTT = 182 °C, $\Delta\sigma_{0.2}$ = 441 MPa	15	75	4	10	75	15	–	–
		16	175	42	55	25	10	–	10
		17	220	63	90	–	–	–	10

metal tested in the temperature range from LSE level to DBT region. Probably, the presence of the given structural component in the fracture is caused by low cooling rate from the tempering temperature, which makes kinetically possible the formation of phosphorus intergranular segregation during heat treatment of steel (at cooling after tempering).

Irradiation of steel causes essential changes in the fracture structure of impact-test specimens at comparable test temperatures. Thus, in specimen fractures tested in the range of temperatures corresponded to USE, in addition to the zones with ductile dimple fracture mode there are the zones with ductile intergranular fracture mode (Fig. 5). Their percentage in the total fracture surface reaches 5–10%. The presence of ductile intergranular component indicates the progress of segregation processes in the steel under irradiation and the occurrence of precipitates with phosphorus segregation on their interface boundaries in locations of former austenite grains. It was shown earlier [1,2] that ductile intergranular fracture mode, which realizes in the case, when grain boundaries are decorated with precipitates with phosphorus segregation on them, that decrease cohesive strength of these boundaries, is an indirect confirmation of segregation presence on radiation-induced precipitates located on the former austenite grain boundaries. In this case the surface of ductile fracture, that envelopes interface boundaries of segregation, follows grain boundaries of the material. As it was shown in [13,14], similar phosphorus segregation is observed on copper-enriched clusters, carbides (carbonitrides) and dislocations. In the general case similar precipitation could present on the grain boundaries in the initial state and/or occur as a result of irradiation or heat treatment.

Fig. 5. The region of ductile intergranular fracture mode in the irradiated specimen from the base metal.

The fact of the occurrence of the zones with ductile intergranular fracture mode in the fractures indicates that atomic decohesion of interface of precipitates that decorate grain boundaries can be at lower stress level, than ductile cleavage.

At decreasing of test temperature down to the values close to DBTT a marked drop is observed of the percentage of ductile and ductile intergranular fracture mode in the total fracture surface of the irradiated specimens. Simultaneously, in the base metal specimens, the occurrence of significant quantity of the zones with brittle intergranular fracture mode is observed (Fig. 2). Their fraction in the total fracture surface reaches 65%. A comparison of the results of earlier fractographic studies for a wide spectrum of VVER-440 steels with different phosphorus content (up to 0.04%) irradiated to fast neutron fluence of $\sim 10^{24}$ n m^{-2} indicates that neutron fluence growth up to $\sim 10^{25}$ n m^{-2} increases fraction of brittle intergranular fracture mode in 2.5–3 times in the specimens from base metal.

Attention is drawn to the fact that there is no brittle intergranular mode in the fractures of the irradiated specimens from weld metal. It should be noted that influence of phosphorus content on the fraction of brittle intergranular component is of complex character. Thus, in VVER-440 base metal specimens, where phosphorus content is, as a rule, significantly less, than in VVER-440 weld metal, after irradiation there are zones with brittle intergranular fracture mode in Charpy specimens [15]. At the same time the similar type of fracture was never seen in Charpy specimens of VVER-440 weld metal. Presumably it is caused by differences in microstructure of these materials. According to the data [15], it might be pointed out that there is a possible reason for higher tendency of Charpy specimens from irradiated VVER-440 base metal to exhibit brittle intergranular fracture in comparison with similar Charpy specimens from irradiated VVER-440 weld metals. As metallographic examination has shown, the microstructure of the base metal is homogeneous and consists of tempered bainite [15]. Compared to base metal, the grains of VVER-440 weld metal consist of tempered bainite and in locations of former high angle austenite grain boundaries there are also grains of excess alpha-ferrite without carbide segregation where intergranular fracture of impact-test specimens occurred mainly [15]. Alloying of steels with Mo and Mn results in a marked drop of phosphorus solubility in alpha-ferrite [16] and, accordingly, causes decreasing of phosphorus segregation on high angle boundaries of the weld (practically lack of phosphorus segregation on high angle boundaries of austenite grains was demonstrated with the use of 3D Atom-Probe in the works [13,14]). At the same time at impact testing of Charpy specimens made from base and weld metals of VVER–1000 with identical homogeneous tempered bainite structure on section of former austenite grains, the occurrence of brittle intergranular fracture in Charpy specimens is of equal probability [15].

Fractographic studies of the specimens from base metal subjected to heat treatment (at 290 °C) without irradiation have revealed the brittle intergranular component in the fracture, however, fraction of this component is much less than in the fractures of irradiated specimens and does not exceed 25 %.

Grain-boundary phosphorus segregation, changing local material properties, does not result in yield strength increase, obviously. However, influence of phosphorus on radiation embrittlement is not only the formation of grain-boundary segregation. It was shown in several publications [1,17] that in many cases phosphorus contribution in radiant embrittlement can be stipulated mostly by hardening mechanism. It can be connected with phosphorus segregation to intragranular precipitates of the second phase – on precipitate/matrix interface.

The modeling of radiation-induced phosphorus segregation at rounded precipitates was carried out in the work [18]. It was shown that in irradiation conditions of VVER-440 pressure vessel steels such segregation occurs at irradiation to fluence of $\sim 10^{23}$ n m^{-2}, at that the density of phosphorus on precipitate boundaries reaches several percents. Also the occurrence of ductile intergranular component in Charpy specimen fractures after irradiation is an indirect confirmation of the fact that under irradiation phosphorus segregation occurs on the interface boundaries of precipitate/matrix. Another mechanism of hardening caused by phosphorus can be its influence on concentration of interstitial loops [19]. Some experimental data [20–22] confirms that growth of phosphorus content in the steel causes irradiation hardening.

The results of electron-microscopy studies of the specimens from base and weld metals in the initial condition and after irradiation to different neutron fluences up to 8.66×10^{24} n m^{-2} are given in Table 3.

The results obtained allow a formulation of the following features of radiation-induced microstructural behavior for base and weld metals of VVER-440 under irradiation up to the neutron fluence of 8.66×10^{24} n m^{-2} ($E > 0.5$ MeV) that is for beyond design operation period (Fig. 6).

As the irradiation dose increases radiation defects become prevailing radiation-induced microstructural components in base and weld metals (Table 3). The radiation defects in the steels are seen as 'black dots' and dislocation loops with 'zero' contrast line (Fig. 7). Analysis of the dark-field images obtained using different effective reflection vectors shows, that all visible defects are dislocation loops. The density of radiation defects in studied base metal irradiated to the over design fluence is $(50–60) \times 10^{15}$ cm^{-3}, and their density in weld metal is $(60–70) \times 10^{15}$ cm^{-3}.

Table 3
The results of electron-microscopy studies of base and weld metals in initial condition and after irradiation to different neutron fluences

No.	Condition	N_{loops}, 10^{15} cm^{-3}	$\langle d\rangle_{loops}$, nm	N_{disk}, 10^{15} cm^{-3}	$\langle d\rangle_{disk}$, HM	$N_{rounded}$, 10^{15} cm^{-3}	$\langle d\rangle_{rounded}$, nm
Base metal (Cu = 0.09%)							
1	Unirradiated	–	–	0.1–0.15	25	–	–
2	Irradiated, $F = 5.3\times10^{23}$ n m^{-2}	6–8	4–6	4–5	20	100–150	2–3
2	Irradiated, $F = 1.3\times10^{24}$ n m^{-2}	30–40	8–9	3–4	23	40–50	3–4
4	Irradiated, $F = 8.66\times10^{24}$ n m^{-2}	50–60	9–10	0.3–0.5	15	10–20	5–6
Weld metal (Cu = 0.03%)							
1	Unirradiated	–	–	0.2–0.3	30	–	–
2	Irradiated, $F = 5\times10^{23}$ n m^{-2}	0.9–1.0	4–5	2–3	11.5	500–700	2–3
2	Irradiated, $F = 1.3\times10^{24}$ n m^{-2}	30–40	7–8	10–15	25	30–40	3–4
4	Irradiated, $F = 8.66\times10^{24}$ n m^{-2}	60–70	10–11	8–10	18–20	10–15	4–5

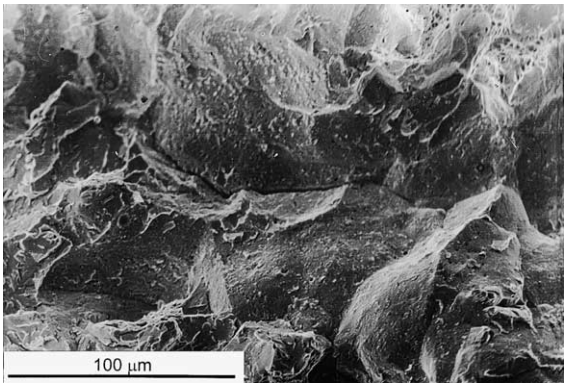

Fig. 6. The region of brittle intergranular fracture mode in the irradiated specimen from the weld metal.

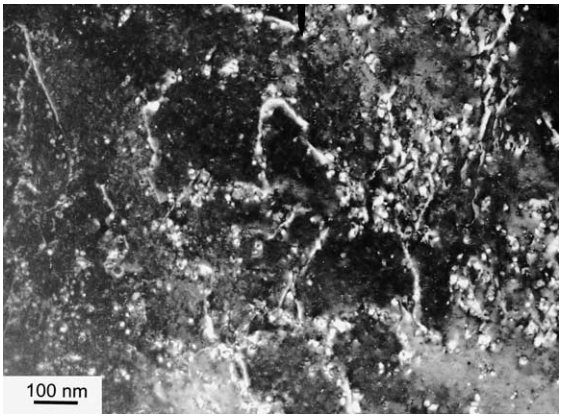

Fig. 7. Radiation defects in the irradiated (fluence of 8.66×10^{24} n m^{-2}) base metal (×100 000).

Under irradiation there is occurrence of new population of disk-shaped precipitates (Fig. 8) (disk-shaped precipitates are $M_7(C,N)_3$ carbonitrides enriched by vanadium [13,14]). As base metal is under irradiation the density of these precipitates decreases a little, and irradiation of weld metal causes some increase of their density and decrease of the mean size.

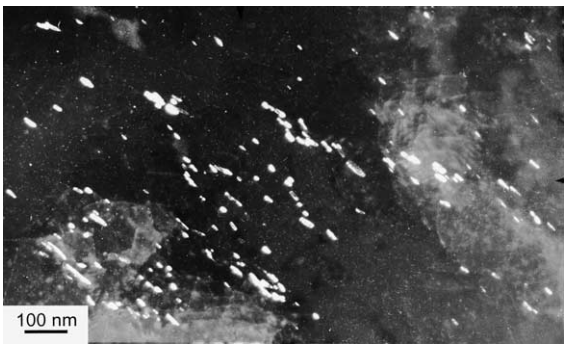

Fig. 8. Disk-shaped precipitates in the irradiated (fluence of 8.66×10^{24} n m^{-2}) base metal (×100).

Irradiation of RPV steels results also in occurrence of rounded precipitates of 2-6 nm (Fig. 9) in them. These precipitates are distributed homogeneously inside grain body of the metal. At early stages of irradiation their density increases sharply, and as irradiation rises the density drops progressively (Table 3). The data [13,14] shows that these precipitates are copper-enriched precipitates, and there is an assumption in the work [23] that their formation is of cascade nature.

A comparison of the results of electron microscopy studies of the given irradiated steels (see Table 3) and the results for RPV obtained earlier [2], the following features connected with neutron fluence increase up to the over design values are noted:

- Increase in the density of radiation defects by more than 50 times and growth of their size by 2 times.
- Decrease in the density of copper-enriched precipitates by about 50 times and growth of their size by 2 times.

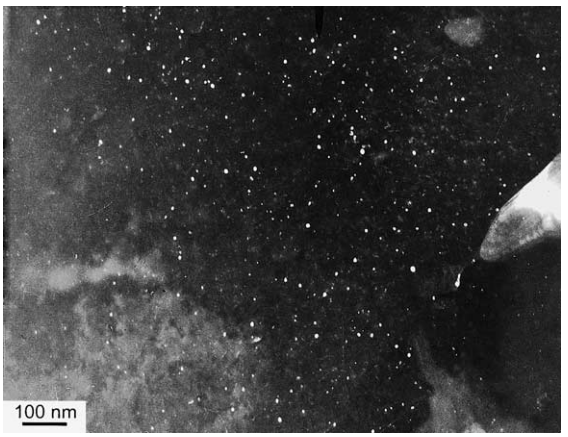

Fig. 9. Copper-enriched precipitates in the irradiated (fluence of 8.66×10^{24} n m^{-2}) base metal (×100000).

4. Discussion

The results obtained show that at the late stages of RPV steels irradiation beyond the design operation period the following structural changes were observed:

1. Occurrence of many radiation defects – dislocation loops.
2. At early stages of irradiation the radiation-induced precipitates dominate, their density being increasing with radiation dose and then decreases; the radiation defects dominate at late stages of irradiation.
3. Fracture mechanism of the base metal at the late irradiation stages was observed to change from transcrystalline to intercrystalline.

First of all, it should be noted the very high (up to 65%) fraction of brittle intergranular component in the fractures of the irradiated base metal. The steel studied is rather pure with regard to impurity elements and, particularly, phosphorus content is 0.011%. Earlier, at studying RPV steels of VVER-440, when fast neutron fluence did not exceed the design fluence ($<10^{24}$ n m^{-2}), it was shown that fraction of brittle intergranular fracture mode, as a rule, was not more than 10–20%.

It is known that in steels with body centered cubic lattice the occurrence of zones with brittle intergranular fracture mode in the fractures is stipulated, as a rule, by the formation of intergranular impurity segregation (principally phosphorus). The occurrence of intergranular phosphorus segregation is observed in RPV steels at irradiation temperature (~270–290 °C), which is much lower than typical temperatures (400–550 °C) for the steel temper brittleness [24]. However, practically in all experimental studies concerning temper brittleness the thermal aging times did not exceed 10000–20000 h [24]. As it is known in the steels there is practically no affinity of phosphorus for grain boundaries (i.e. it equals 0) at the temperatures higher than 600–650 °C and the affinity increases with temperature decrease (Fig. 10). Nickel alloying of the steel clear causes the non-monotonic increase of phosphorus affinity for the grain boundaries in the steels as temperature decreases (Fig. 10). At rather low temperatures the formation of intergranular phosphorus segregation is controlled only by kinetic factor (Fig. 11), therefore at the given tempering time the level of intergranular phosphorus density in the beginning increases with tempering temperature decrease, then has a maximum and further decreases [24]. Hence, prolongation of heat treatment (by more than an order of values as compared to the basic experimental data file obtained for temper brittleness) can change considerably a character of temperature dependences concerning evolution of intergranular phosphorus segregation especially at low temperatures.

According to the above-mentioned, fractographic studies of the base metal specimens from the thermal set subjected to isothermal ageing (3520 effective days at 290 °C) without irradiation were carried out. These studies allowed to separate the contribution of radiation component in occurrence of intergranular segregation from temper brittleness effect at the working temperatures of ~270–290 °C and equivalent time – about 100000 h. A comparison of the fractions with brittle intergranular fracture mode in the specimens from the thermal set and irradiated base metal (see Table 2) shows that in the specimens irradiated the fraction is by three times less than in the specimens of the thermal set.

It was shown [25] that thermal ageing of Cr–Ni–Mo steel at ~275 °C for 60000 h causes increase in the density of intergranular phosphorus in 10 times less, than

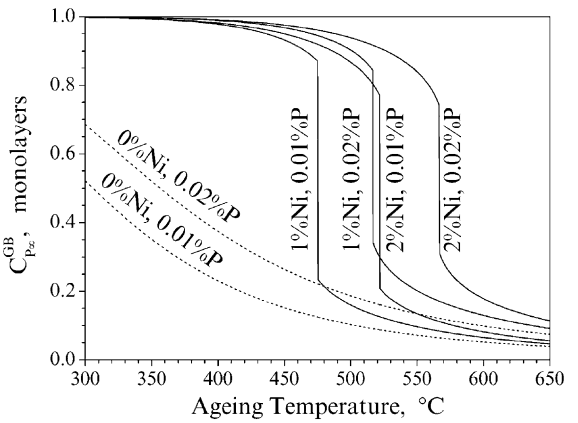

Fig. 10. Equilibrium phosphorus concentration as a function of ageing temperature.

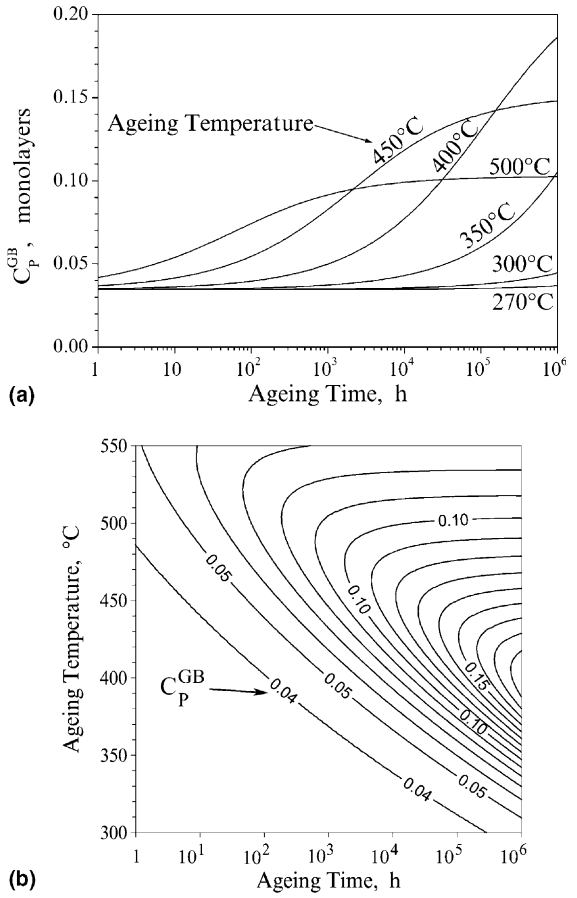

Fig. 11. The dependence of the grain boundary phosphorus segregation kinetics on aging temperature for the steel with 0% Ni and 0.01% P.

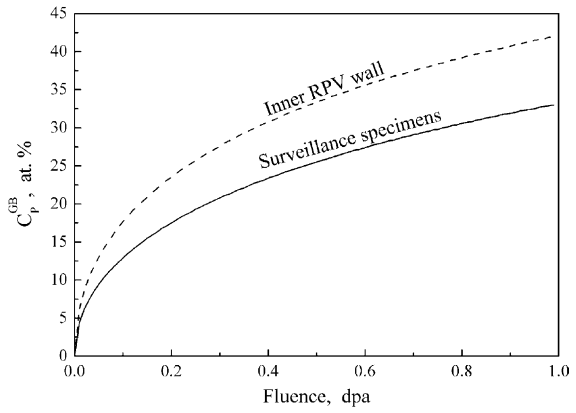

Fig. 12. Calculation for phosphorus accumulation on the grain boundaries of base metal (0.01% P) in the inner RPV wall ($K = 3 \times 10^{-10}$ dpa/s) and in the surveillance specimens ($K = 2.8 \times 10^{-9}$ dpa/s) at 270 °C.

after irradiation to fast neutron fluence of 6.2×10^{23} n m^{-2}.

As noted above, the essential contribution of brittle intergranular mode in the specimens fractures after irradiation, connected with phosphorus segregation on the grain boundaries, is detected only in the base metal, and is not observed in the weld metal, that is caused by essential microstructural differences of these materials. Therefore, for the base metal it is important to estimate accumulation of phosphorus on the grain boundaries under irradiation and its possible contribution to radiation embrittlement. The kinetics of phosphorus accumulation on the grain boundaries, taking into account radiation-accelerated diffusion of phosphorus by vacancy and interstitial mechanisms and radiation-induced segregation to the grain boundaries, was studied in [26,27]. The results for RPV inner wall and the surveillance specimens studied in the present work are presented in Fig. 12. It is seen that at a temperature of 270 °C irradiation accelerates phosphorus enrichment of the grain boundaries. At identical irradiation doses phosphorus enrichment of the grain boundaries in the surveillance specimens is lower, than on the inner surface of the pressure vessel.

As mentioned above, in VVER-440 RPV steels at rather small radiation doses the matrix hardening is connected, mainly, with the formation of copper-enriched precipitates, not dislocation loops, and it is possible to describe it sufficiently by the existing standard reference dependence specified in the Russian Guide [8]. As follows from the calculations made (Fig. 12), the phosphorus accumulation on the grain boundaries of base metal forms rather slowly. Therefore, the mechanism of intergranular embrittlement connected with this accumulation could be revealed and considered at rather high radiation doses.

The model of embrittlement similar to the one used in the works [26,28] was developed in [27], and it considers both mechanisms mentioned. The first mechanism connected with the matrix hardening causes yield strength σ_y increase and a DBTT shift ΔT_1, the second one connected with phosphorus segregation and lowering of intergranular cohesion causes decrease of intergranular fracture stress σ_F and ΔT_2 connected with it. If both mechanisms operate, in assumption of additivity the total DBTT shift $\Delta T = \Delta T_1 + \Delta T_2$ [27,28]. As can be concluded from [29] the assumption of additivity can be considered as very rough since matrix hardening and decrease of grain boundary cohesion due to phosphorus segregation are synergistic phenomenon.

Under irradiation the value of σ_y increases, and σ_F decreases. Since some critical dose F_c, $\sigma_F \leqslant \sigma_c$, where σ_c is a stress of ductile intergranular fracture. After that the mechanism of intergranular embrittlement contributes into ΔT, and this contribution increases with fluence growth. As experimental studies of reversible

temper brittleness for low alloyed steels [3,24] shows (conditions of thermal ageing), a DBTT shift ΔT_2, connected with phosphorus segregation on the grain boundaries, is proportional to $\Delta\sigma_F$ which one in turn is proportional to ΔC_P^{GB} that is a change of phosphorus density on the grain boundaries.

Neglecting the synergistic effect of the matrix hardening, that is usually considered to be responsible for radiation embrittlement, and decrease of grain boundary cohesion due to phosphorus segregation and taking into account the standard reference dependence specified in the Russian Guide [8] it can be suggested the following equation for radiation-induced DBTT shift:

$$\Delta T_F = A_F F^{1/3} + \delta \cdot A_P (C_P^{GB}(F) - C_P^{GB}(F_0)), \quad (1)$$

where F_0 is the threshold fluence for phosphorus segregation effect: $\delta = 0$ when $F < F_0$ and $\delta = 1$ when $F \geqslant F_0$. The dependence $C_P^{GB}(F)$ is calculated by modeling of phosphorus accumulation on the grain boundaries, the value of F_0 is considered as adjusted parameter.

The results of the calculation by the model suggested together with experimental data are presented in Fig. 13. The dose is given in displacement per atom (dpa) on the basis of 10^{24} n m^{-2} ($E > 0.5$ MeV) ≈ 0.1 dpa, and as F_0 the fluence of 2×10^{24} n m^{-2} ($E > 0.5$ MeV) is chosen. The proportionality coefficient A_P is chosen as 7 (°C/at.%P) that agrees with the experimental data [28] for dependence $\Delta T_2(C_P^{GB})$ in thermal ageing conditions. The coefficient α that equals ratio between phosphorus density on the grain boundaries before irradiation to its content in the matrix and it takes into account possible phosphorus adsorption on the grain boundaries during preliminary heat treatment.

It is seen that the model dependence (1) suggested describes satisfactorily the data at high radiation doses. It should be noted that this dependence also describes the data obtained on the surveillance specimens from base metals of other NPP: Armenia Unit 2 and Rovno Unit 2 reactors [27]. As regard to the weld metal, phosphorus accumulation on the grain boundaries in it occurs much less. Therefore, in weld metal at high neutron fluences there is only intragranular embrittlement connected with the formation of intragranular solute segregation and matrix hardening by interstitial loops.

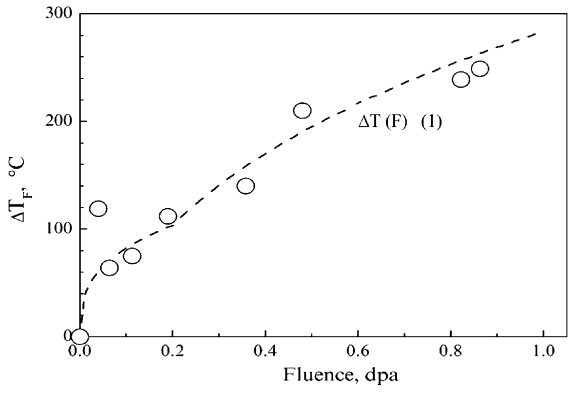

Fig. 13. Comparison of calculated DBTT dependence on damage dose for the base metal with the experimental data.

TEM studies of the specimens irradiated to neutron fluence of 8.66×10^{24} n m^{-2} have demonstrated considerable increase in the density growth of dislocation loops as compared to the steels studied earlier irradiated to design end-of-life neutron fluence (see Table 3). High density of formed radiation defects causes high radiation hardening of the matrix (essential yield strength increase: $\Delta\sigma_{0.2} = 442$ MPa is observed, see Table 2), that, in its turn, at other conditions being equal promotes change in strength balance between grain body/grain boundaries to the grain body. At impact testing it makes more preferable not transcrystalline fracture, but intergranular fracture of the specimens [29,30]. Therefore, increase of intergranular fraction in the fractures of the specimens irradiated to high neutron fluence happens due to synergetic interaction of grain body hardening and radiation-induced intergranular phosphorus segregation.

Recovery annealing of RPV steels irradiated at the temperatures of <475 °C (i.e. at the temperature of recovery annealing that is used for safe life prolongation of the nuclear reactor pressure vessels) do not result in complete recovery of the radiation-induced structural changes [2]. This annealing causes nearly total disappearance of radiation defects, considerable but not complete density recovery of radiation-induced precipitates and intragranular phosphorus segregation. They do not cause decrease a level of intergranular phosphorus segregation and even can promote its increase. However, essential recovery of yield strength (matrix hardening decrease) as a result of recovery annealing at constant intergranular segregation level can lead to grain body fracture as more preferable.

Fractographic studies have shown that fraction of ductile intergranular fracture mode in the fractures of base metal specimens irradiated is 5%, and in the fractures of weld metal specimens it is 10% (see Table 2). It should be noted that fraction of ductile intergranular fracture mode in the specimen fractures of any steel does not depend directly on the level of phosphorus segregation on the interface of the corresponding precipitates. The fraction is estimated, mainly, by surface share of grain boundaries that are decorated by these precipitates in the total grain boundary surface. Observations with the use of TEM method show that precipitate decoration of the boundaries occurs extremely irregular. This fact makes principle difference between ductile intergranular fracture and brittle intergranular fracture. Nevertheless, small fraction of ductile intergranular fracture

mode in the irradiated steel studied as compared to analogue fraction in RPV steels studied earlier (up to 15% in the steels irradiated to lower neutron fluence $<10^{24}$ n m^{-2} [2]), probably together with low copper content, is stipulated by total decrease in the density of radiation-induced precipitates, that are support for intragranular interface segregation.

As follows from TEM data (Table 3), the density of radiation-induced copper-enriched precipitates in the RPV steels irradiated to over design fluences more than in 50 times lower than at early radiation stages. Such behavior of the copper-enriched precipitate density can be caused as by re-dissolution of copper-enriched precipitates due to dispersions by the fast neutrons (originated from atom cascade collisions) of atoms forming precipitates into the matrix as by radiation-induced coalescence (diffusion re-dissolution) at relatively high radiation doses. The observed peculiarities of this process can be connected with complicated composition of the segregation and their evolution under irradiation.

The dependences of density for interstitial loops, rounded and disk-shaped precipitates and their sizes on fast neutron fluence are presented in Figs. 14 and 15. Here there are presented also predictions of the coalescence theory (diffusive re-dissolution) for copper-enriched (rounded) precipitates according to which time dependences of density and size have the following form: $N_{Th} \sim t^{-1}$, $d_{Th} \sim t^{1/3}$. It is seen that the theory predictions agree satisfactorily with the experimental data for base metal and disagree in a case of weld metal. It should be noted, that in the classic coalescence theory it is supposed that volume of precipitates are constant. As follows from Table 3, this condition is satisfied for rounded precipitates in base metal. At the same time, as estimations show, in a case of weld metal there is essential volume decreasing for these precipitates in an interval of fluences of 5.3×10^{23}–1.3×10^{24} n m^{-2}, after this dose the volume remains constant.[1] Another assumption of the coalescence theory is stability of diffusion constant and it also can be not satisfied under irradiation, as the constant of radiation-accelerated copper diffusion depends essentially on the density of point defects. This density is determined by re-combination coefficient and by sinks density, which varies with neutron fluence increase. As estimations show, at the fluences of $>10^{23}$ n m^{-2} this density can exceed essentially (by an order) the general dislocation density in RPV materials ($\sim 10^{10}$ cm^{-2}).

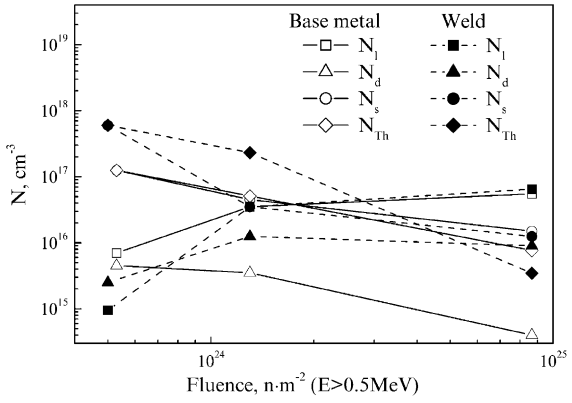

Fig. 14. The density of rounded (N_s), disk-shaped (N_d) precipitates and dislocation loops (N_l) as a function of fast neutron fluence together with prediction of the coalescence theory for rounded precipitates (N_{Th}) for base and weld metals.

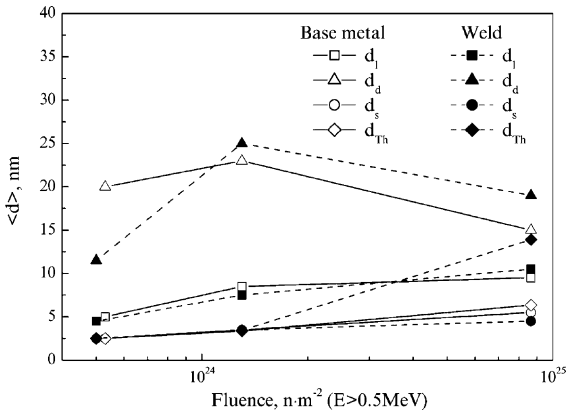

Fig. 15. Average size of rounded (d_s), disk-shaped (d_d) precipitates and dislocation loops (d_l) as a function of fast neutron fluence together with prediction of the coalescence theory for rounded precipitates (d_{Th}) for base and weld metals.

Typical for radiation-induced structural changes in both base and weld metals after irradiation up to the over design fluence of $\sim 10^{25}$ n m^{-2} is domination of radiation defects – dislocation loops as compared to other radiation-induced structural components (disk-shaped and copper-enriched precipitates, see Table 3).

In the work [1] the different mechanisms and their relative contribution to radiation embrittlement (i.e. DBTT shift estimated at impact tests) of RPV steels were studied carefully. There was shown that radiation embrittlement is stipulated, first of all, by the formation of intragranular phosphorus segregation and in lesser degree by complex of effects, which is accepted to name shortly as radiation hardening. The contribution of intergranular phosphorus segregation in radiation embrittlement of RPV steels was evaluated as not more than 10–20%.

[1] It also can be stipulated by the fact that in weld metal there are a lot of ultrafine precipitates, which cannot be detected by TEM studies because their sizes are out of the method resolution.

The complex structural and fractographic studies allow more clear understanding of indicated above mechanisms effect, that, as a whole, results in radiation embrittlement of RPV steels at late stages of irradiation.

The dependencies of DBTT shift and yield strength on radiation dose increase for the studied base and weld metals of VVER-440 are shown in Figs. 1 and 2. Comparison of TEM-studies results and these dependencies shows that there is a correlation between radiation-induced structural changes and character of yield strength increase in the steel. Increase of $\Delta\sigma$ at first stages of irradiation (up to $(3–4)\times10^{23}$ n m^{-2}) is stipulated by marked growth of radiation-induced precipitate density that prevails over density growth of radiation defects. At further increase of radiation dose the density of precipitates decreases, and the density of radiation defects is not yet great enough, that causes slowing-down of $\Delta\sigma$ growth and even its lowering. At late stages of irradiation to fluences close for design and beyond design operation period, the marked growth of yield strength, mainly, is stipulated by formation of many radiation defects – dislocation loops. There is a change of the mechanism that controls radiation hardening of the material. Such behavior of yield strength fits theoretical concept.

According to the existing theory for hardening (see, for example, discussion in [26]), the contribution of this defect type into the yield strength increase $\Delta\sigma$ can be presented as the following:

$$\Delta\sigma = \alpha_i MGb\sqrt{Nd}, \tag{2}$$

where G is shear modulus, b is Burgers vector, M is Taylor factor, N and d are density and size of the given defect type, and α is corresponding to them hardening coefficient.

It should be noted that the value of α_i was evaluated only for rather large defects [26]. It is not known for ultra small defects with sizes less than TEM resolution limits, though in [26] there was noted a tendency for α_i value to decrease with d decreasing. In the work [31] there was made a comparison of $\Delta\sigma$ experimental values after irradiation of several austenitic steels in ORR at the temperatures 60–400 °C up to 7 dpa with calculated by Eq. (2) values using electron-microscopy data concerning densities and sizes of different lattice defects. In this work the satisfactory agreement of $\Delta\sigma$ calculated and experimental values for the temperatures of ~300 °C was obtained. At the temperature of ~400 °C, the calculated value of $\Delta\sigma$ is smaller, as compared to experimental. According to [31] it is connected with possible neglect of the contribution of invisible defects, or with influence of radiation-induced segregation of alloy components to the defects on the value of α_i.

For ultrafine defects of a lattice observed in RPV steels such as precipitates and loops the precise values of hardening coefficients are not known. Maximum possible contribution to the hardening of rounded and disk precipitates, and also contribution of dislocation loops to radiation hardening of base and weld metals together with experimental data from Table 2 are shown in Fig. 16. The contributions were evaluated using data of Table 3 by Eq. (2) when maximum of hardening coefficients is assumed to be: $\alpha_i M \approx 1$ (see [26]). Using data of Fig. 16 it is possible to conclude that ultrafine copper-enriched precipitates are, apparently, weak hardening barriers ($\alpha_i M \ll 1$). At the same time the coefficient of hardening by dislocation loops grows with their size growth, so that at maximum neutron fluence their contribution can define completely the yield strength increase measured.

The differences observed in dose dependences of yield strength and DBTT shift (see Figs. 1 and 2) can be attributed to other mechanisms of radiation embrittlement, i.e. by the formation and evolution of intragranular and intergranular phosphorus segregation.

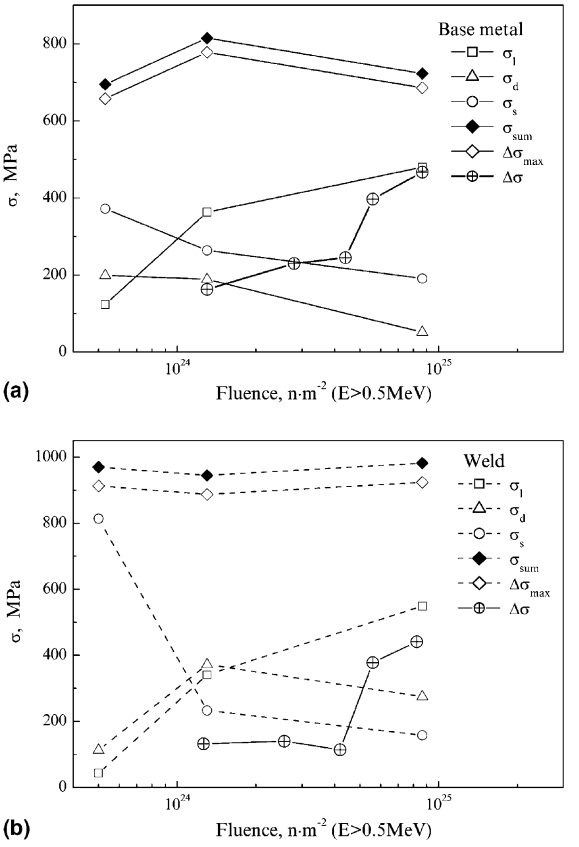

Fig. 16. Comparison of predicted by Eq. (2) maximal contribution in the hardening of rounded (σ_s) and disk-shaped (σ_d) precipitates, interstitial loops (σ_l), summarized contribution (σ_{sum}), and also predicted maximal hardening ($\Delta\sigma_{max}$) with the experimentally observed values ($\Delta\sigma$) for base metal (a) weld metal (b).

Hence, the resulting effect of DBT temperature shift is stipulated by synergetic effect of the radiation hardening mechanisms and impurity segregation on the interface and the grain boundaries. At that acceleration of radiation embrittlement at late stages of irradiation (the values of fast neutron fluence more than $\sim 4 \times 10^{24}$ n m^{-2}) is stipulated by intensive increase in the dislocation loops density at continuous growth of phosphorus segregation level on the interface and the grain boundaries.

5. Conclusion

Comparative results, obtained in this work, of complex structural studies for VVER-440 base and weld metals before and after irradiation up to the fast neutron fluences for beyond design operation period (8.66×10^{24} n m^{-2}) allow one to make the following conclusions about structural features and the mechanisms responsible for radiation hardening and embrittlement:

1. Irradiation causes a complex of structural changes: the formation of radiation defects, phase changes with the occurrence of two types of ultrafine precipitates, the formation of intragranular and intergranular impurity segregation.
2. At early stages of irradiation the radiation-induced precipitates dominate, at first their density increases with radiation dose, and then decreases; the radiation defects dominate at late stages of irradiation.
3. As reaching the design values of fast neutron fluence ($\sim 4 \times 10^{24}$ n m^{-2}) there is change in relative contribution of the mechanisms controlling radiation hardening and embrittlement of the RPV steel. Increase in dislocation loops density was shown to provide the dominant contribution to radiation hardening at the late irradiation stages (after reaching the double design and-of-life neutron fluence of $\sim 4 \times 10^{24}$ n m^{-2}). Fracture mechanism of the base metal at those stages was observed to change from transcrystalline to intercrystalline.

Acknowledgement

The work was carried out at support of the Russian Foundation for Basic Research under Project No. 01-02-16822.

References

[1] B.A. Gurovich, E.A. Kuleshova, Yu.A. Nikolaev, Ya.I. Shtrombakh, J. Nucl. Mater. 246 (1997) 91.
[2] B.A. Gurovich, E.A. Kuleshova, K.E. Prihodko, O.V. Lavrenchuk, Ya.I. Shtrombakh, J. Nucl. Mater. 264 (1998) 333.
[3] C.A. English, S.R. Ortner, G. Gage, W.L. Server, S.T. Rosinski, in: Effects of Radiation on Materials: 20th International Symposium, ASTM STP 1405 (2001) 151.
[4] B.A. Gurovich, E.A. Kuleshova, Ya.I. Shtrombakh, O.O. Zabusov, E.A. Krasikov, J. Nucl. Mater. 279 (2–3) (2000) 259.
[5] V.A. Pechenkin, I.A. Stepanov, Yu.V. Konobeev, in: Effects of Irradiation on Materials: 20th International Symposium, ASTM STP 1405 (2001) 174.
[6] Ya.I. Shtrombakh, Doctoral thesis, RRC 'Kurchatov Institute', Moscow, 1998, p. 240.
[7] V.I. Levit, Yu.N. Korolev, Ph. Tipping, R.N. Lessa, in: Effects of Radiation on Materials: 18th International Symposium, ASTM STP 1325 (1999).
[8] Guide for strength analysis of the equipment and pipelines of nuclear power units, PNAE G-7-002-86, M. Energoatomizdat, 1989.
[9] The evaluation technique of critical brittleness temperature for reactor pressure vessel materials using test results of subsize specimens, RRC KI Report, Inv. No. 60/854, 1992.
[10] Yu.N. Korolev, Ya.I. Shtrombakh, Yu.A. Nikolaev, Ye.A. Krasikov, P.A. Platonov, in: M.A. Sokolov, J.D. Landes, G.E. Lucas (Eds.), Small Specimen Test Techniques: Fourth Volume, ASTM STP 1418 (2002) 151.
[11] S.A. Saltykov, Stereometric metallography, Metallurgy, Moscow, 1976.
[12] P.M. Kelly, A. Jostsons, R.G. Blake, J.G. Napier, Phys. Status Solidi (A) 31 (1975) 771.
[13] P. Pareige, B. Radiguet, A. Suvorov, M. Kozodaev, E. Krasikov, O. Zabusov, J.P. Massoud, Application of the 3D Atom-Probe to the Study of the Re-embrittlement of a VVER 440 Steel Presentation on 48th International Field Emission Symposium, 7–11 July 2002, Lyon, France.
[14] O.O. Zabusov, E.A. Krasikov, M.A. Kzodaev, A.L. Suvorov, P. Pareige, B. Radiguet, Report at 15th International Conference on Physics of Radiation Phenomena and Radiation Materials Science, Alushta, 2002.
[15] E.A. Kuleshova, B.A. Gurovich, Ya.I. Shtrombakh, D.Yu. Erak, O.V. Lavrenchuk, J. Nucl. Mater. 300 (2002) 127.
[16] I.I. Novikov, The theory of metal heat treatment, Metallurgy, Moscow, 1978, p. 392.
[17] B.A. Gurovich, Yu.N. Korolev, E.A. Kuleshova, Yu.A. Nikolaev, Ya.I. Shtrombakh, in: R.K. Nanstad, M.L. Hamilton, F.A. Garner, A.S. Kumar (Eds.), Effects of Radiation on Materials, ASTM STP 1325 (1999) 271.
[18] I.A. Stepanov, V.A. Pechenkin, Yu.V. Konobeev, in: Effects of Radiation on Materials: 21st International Symposium, ASTM STP 1447 (2003).
[19] G.R. Odette, G.E. Lucas, JOM 53 (7) (2001) 18.
[20] A.V. Nikolaeva, Yu.A. Nikolaev, Yu.R. Kevorkyan, A.M. Kryukov, Yu.N. Korolev, Atom. Energy. 88 (4) (2000) 271.
[21] Y.I. Shtrombakh, Int. J. Press. Vess. Piping 79 (8-10) (2002) 619.
[22] A.D. Amaev, A.M. Kryukov, V.I. Levit, M.A. Sokolov, in: L.E. Steele (Ed.), Radiation Embrittlement of

Nuclear Reactor Pressure Vessel Steels, ASTM STP 1170 (1993) 9.
[23] P.A. Platonov, Yu.A. Nikolaev, Ya.I. Shtrombakh, Irradiation Embrittlement and Mitigation, Proceeding of the IAEA Specialists Meeting, United Kingdom, 14–17 May 2001.
[24] L.M. Utevsky, E.E. Glikman, G.S. Kark, Reversible temper brittleness of ferrous steels and alloys, Metallurgy, Moscow, 1985, p. 10.
[25] A.V. Nikolaeva, Yu.A. Nikolaev, Yu.R. Kevorkyan, O.O. Zabusov, Atom. Energy. 91 (5) (2001) 343.
[26] G.E. Lucas, J. Nucl. Mater. 206 (1993) 287.
[27] V.A. Pechenkin, Yu.V. Konobeev, I.A. Stepanov, Yu.A. Nikolaev, in: Effects of Radiation on Materials: 21st International Symposium, ASTM STP 1447 (2003).
[28] C.J. Bolton, J.T. Buswell, R.B. Jones, R. Moskovic, R.H. Priest, in: Effects of Radiation on Materials: 17th International Symposium, ASTM STP 1270 (1996) 103.
[29] J.-S. Wang, P.M. Anderson, Acta Metall. Mater. 39 (1991) 779.
[30] P.M. Anderson, J.R. Rice, Scr. Metall. 20 (1986) 1467.
[31] M.L. Grossbeck, P.J. Maziasz, A.F. Rowcliffe, J. Nucl. Mater. 191–194 (1992) 808.